Steric effects which determine the conformational preferences and stereodynamic processes of aryl fluorenyl ketones†

Daniele Casarini,*[a] Lodovico Lunazzi[b] and Andrea Mazzanti*[b]

Received 19th December 2008, Accepted 29th January 2009
First published as an Advance Article on the web 28th February 2009
DOI: 10.1039/b822874d

The stereodynamic processes and conformational preferences of two classes of aryl fluorenyl ketones have been investigated by means of dynamic NMR spectroscopy, DFT calculations and X-ray diffraction. When the aryl substituent has two hydrogens in the *ortho* positions, its rotation is independent of that of the fluorene ring. In contrast, if the two *ortho* hydrogens are replaced by the bulkier methyl groups (*e.g.* mesityl fluorenyl ketones), the motion of the aryl ring interacts with the fluorene, and the two rings rotate in a correlated manner.

Introduction

Restricted rotation processes occurring in 9-fluorenyl derivatives have been detected by NMR spectroscopy, and the corresponding barriers, as well as the structures of the preferred conformers, determined.[1–3] Recently it has been also shown that the fluorenyl motif can be used in the design of molecular motors.[4] Examples of dynamic processes have been encountered in 9-aryl[1–3] and 9-alkyl[5] fluorenyl compounds, where a single rotation pathway has been found to take place. On the other hand, in the arylfluorenylketones, more than one rotation pathway should be detectable, in principle. To verify this prediction, a series of arylfluorenylketones have been synthesized (Scheme 1) and the corresponding internal motions investigated by dynamic NMR spectroscopy, with the support of theoretical calculations. These processes are expected to give rise to conformers with different symmetries as well as distinct stereodynamic processes, depending on the steric properties of the substituents.

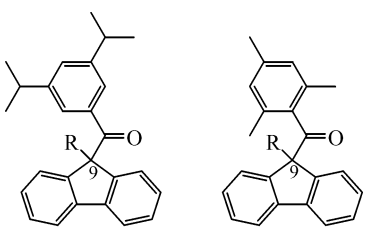

Scheme 1

[a]*Department of Chemistry, University of Basilicata, via N. Sauro 85, Potenza, 85100, Italy. E-mail: casarini@unibas.it*
[b]*Department of Organic Chemistry "A. Mangini", University of Bologna, Viale Risorgimento 4, Bologna, 40136, Italy. E-mail: mazzand@ms.fci.unibo.it; Fax: +39-051-2093654*

† Electronic supplementary information (ESI) available: DFT-calculated geometries of **1**, NOE spectra of **2** and **4**, ^{13}C and ^{1}H VT spectra of **3**, VT spectra and simulations of **1–3**, stereomutation pathway of **4**, X-ray diffraction data and CIF files of **3** and **5**, experimental procedures for the preparation of **1–5** and their intermediates; ^{1}H and ^{13}C NMR spectra of **1–5** and their intermediates, analytical HPLC traces and computational data for **1–5**. See DOI: 10.1039/b822874d

Results and discussion

The variable-temperature ^{1}H spectrum (at 600 MHz) of compound **1** shows how the single line of the hydrogen in position 9 broadens considerably and eventually splits, at –147 °C, into two lines with a 94 : 6 intensity ratio. Similar changes occur for the signals of the CH and of the methyl groups of the isopropyl substituents. In the major conformer both signals are further split into 1 : 1 pairs, as in Fig. 1 (this additional feature will be discussed subsequently).

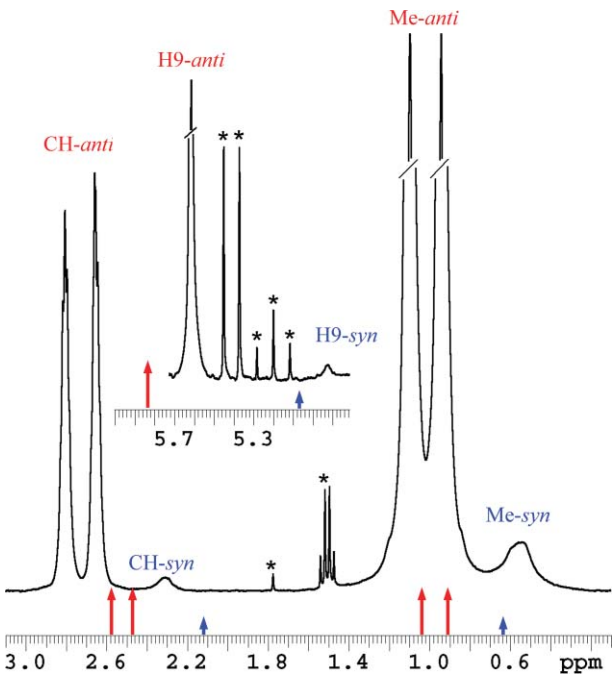

Fig. 1 ^{1}H NMR spectrum of the aliphatic region of **1** (600 MHz in $CHF_2Cl/CHFCl_2$, at –147 °C, with the stars indicating the solvent impurities). The arrows represent the computed shifts (all moved 0.35 ppm upfield); those of the *syn* conformer (shorter arrows) lie consistently upfield of its *anti* companion (longer arrows).

The observation of signals of unequal intensity proves that the molecule adopts two conformations with different stability. A complete molecular mechanics conformational search[6]

(see Experimental Section) identifies the existence of two low energy conformers with similar energies, the difference being 0.0 in the MMX[7] and 1.1 kcal mol^{-1} in DFT computations (B3LYP/6-31G(d) level[8]). These ground states are labelled **1**-*syn* (C_s symmetry) and **1**-*anti* (C_1 symmetry) in Scheme 2. The distance between H-9 and H-1,8 in the **1**-*anti* form is larger than the average distance between H-9 and H_{ortho},[9] therefore the NOE at the H_{ortho} protons, when H-9 is irradiated, is expected to be greater than that at the H-1,8 signal, whereas in **1**-*syn* it is expected to be smaller.[9]

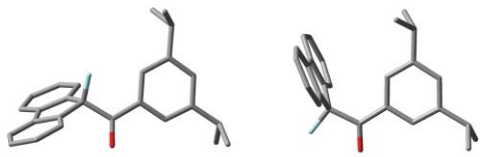

1-*anti* (C_1) **1**-*syn* (C_s)

Scheme 2 DFT-computed structures of the *syn* and *anti* conformers of **1**. All the hydrogens have been omitted, except that in position 9 of fluorene. The dihedral angles H9–C9–C–O are 148° and 0° in **1**-*anti* and **1**-*syn*, respectively; the C=O and phenyl ring are coplanar in both conformers.

An NOE experiment was then carried out at a temperature (–80 °C) where the two conformers are still in rapid exchange.[10] As shown in Fig. 2, irradiation of the H-9 line yields a NOE effect on the signal of the *ortho* hydrogens (H_{ortho})[11] of the substituted phenyl

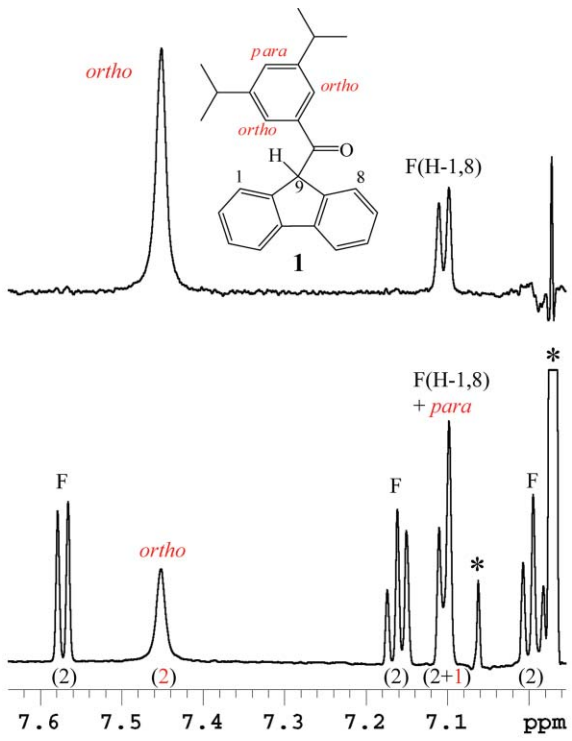

Fig. 2 Bottom: ^{1}H 600 MHz spectrum (at –80 °C in $CHF_2Cl/CHFCl_2$) of the aromatic region of **1**. The letter F identifies the fluorene signals and *ortho*, *para* the corresponding signals of the *meta*-diisopropylphenyl moiety. The numbers in parentheses are the integrated intensities and the stars identify the solvent (and its ^{13}C satellite) signals. Top: NOE spectrum obtained by irradiating H-9 (5.50 ppm). The enhancement of the *ortho* signal is 3.1 times larger than that of the 1,8 fluorene signal, *i.e.* F(H-1,8).

group that is larger (by a factor of 3.1) than that experienced by the hydrogens in positions 1,8 of the fluorenyl moiety, *i.e.* F(H-1,8). Likewise, irradiation of the signal of the *ortho* hydrogens (H_{ortho}) yields a NOE on the H-9 line 2.5 times larger than that due to the irradiation of the signals of the 1,8 hydrogens of fluorenyl *i.e.* F(H-1,8)[12] The fact that the two NOE approaches yield essentially the same result (2.5 : 1 is very close to 3 : 1 within the experimental uncertainty of ±0.3) means that the major conformer must have a structure where H-9 is closer to the *ortho* (H_{ortho}) than to the F(H-1,8) hydrogens.[9] On this basis the *anti* structure should be assigned to the more populated conformer.

The assignment based upon the NOE experiment is at variance with the DFT-computed energies, in that the *syn* conformer has an energy 0.77 kcal mol^{-1} lower than the *anti* conformer. At the higher B3LYP/6-311++G(2d,p) level[8] the ZPE-corrected energies yield a $\Delta G^\circ = -0.42$ kcal mol^{-1} ($G^\circ_{syn} - G^\circ_{anti}$), while the experimentally determined ratio at –147 °C corresponds to a $\Delta G^\circ = 0.69$ kcal mol^{-1}. Therefore, the discrepancy is still about 1.1 kcal mol^{-1}. In recent years it has been shown[13] that the B3LYP density functional occasionally fails to provide accurate energies. For this reason, alternative functionals [PBE1PBE/6-31G(d), M05-2X/6-31G(d)] and *ab initio* methods [RHF(full)/6-31G(d), RHF/cc-pVDZ, MP2(full)/6-31G(d), CISD/6-31G(d)] were employed. In all the DFT calculations the *syn* conformer was more stable than the *anti* by a difference larger than that obtained with both the B3LYP calculations, while the best agreement with experimental data was obtained with the simpler RHF(full)/6-31G(d) calculation (energy difference = 0.04 kcal mol^{-1}), in which electronic correlation is not considered (see ESI† for a summary). As a second attempt, B3LYP calculations were performed in the presence of a solvent. Because the freon mixture used for NMR experiments was very difficult to parametrize, dichloromethane was chosen as mimic solvent, and calculations were performed using the Polarizable Continuum Model and the 6-311++G(2d,p) basis set. In this case the energy difference reduces to 0.10 kcal mol^{-1}, but the *syn* conformer is still calculated to be more stable than the *anti*. The present case can be therefore considered an additional example of a discrepancy between the computed and experimental energy difference.[13] A possible reason could be due to the fact that calculations (especially when carried out for the isolated molecule, but possibly also in very polar solvents) might overestimate a stabilizing edge-to-face aromatic–aromatic interaction between the *ortho* hydrogens of the phenyl ring and the π-surface of the fluorenyl residue (for instance in the case of compound **3** the X-ray structure indicates that this distance is 2.4 Å).

An alternative approach for assigning the conformers uses the computed and experimental NMR shifts: in the present case this calculation supports the assignment derived from the NOE experiment. As shown in Fig. 1 the shifts of the aliphatic hydrogens of the *syn* conformer (shorter arrows) are computed to be upfield from those of the *anti* conformer (longer arrows), which indicates that the more intense downfield signals are for the more populated *anti* conformer.

To account for the existence of the unequally populated *anti* and *syn* conformers, the fluorenyl–CO bond rotation must be frozen at low temperature. The line shape simulation of Fig. 3 indicates that the barrier for this process, which interconverts the major into the minor conformer and exchanges the two isopropyl signals of the major conformer, is 6.8 kcal mol^{-1} (Table 1). This value agrees

Table 1 Barriers (±0.2 kcal mol^{-1}) measured for the observed dynamic processes of **1** and of **3–5**. The DFT-computed values are reported in parentheses

Compd	Type of process	Barrier/kcal mol^{-1}
1	Fluorenyl–CO rotation (*anti* to *syn* exchange)	6.8 (6.7)
3	Isopropyl–C9 rotation	7.9 (7.8)
4	Mesityl–CO rotation	4.4 (4.3)
	Isopropyl–C9 rotation	6.9 (6.2)
5	*Syn* (*trans*) to *syn* (*cis*) interconversion	6.0 (4.8)

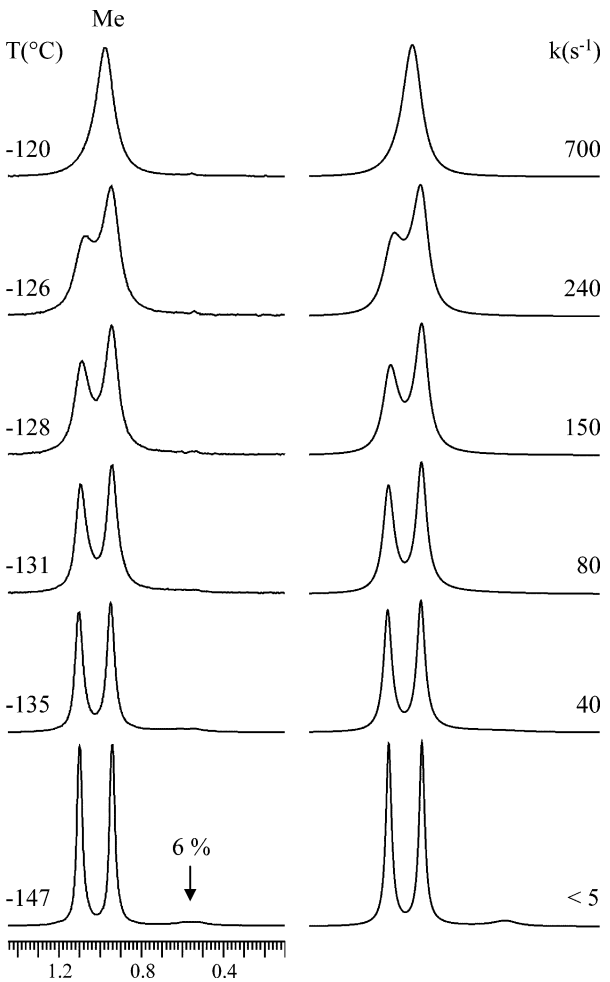

Fig. 3 Temperature dependence of the isopropyl methyl signals (600 MHz in $CHF_2Cl/CHFCl_2$) of compound **1** (the doublet splitting due to the *J* coupling with CH is obscured by the broad line width at low temperature). On the right the simulation obtained with the reported rate constants (see text and ref. 15).

well with the computations that predict a fluorenyl–CO rotation barrier of 6.7 kcal mol^{-1}.

As mentioned above, the isopropyl signals of the major conformer are split in a 1 : 1 ratio (Fig. 1). This means that, as well as the fluorenyl–CO bond, the aryl–CO bond rotation in the *anti* form is also frozen. In contrast, the corresponding isopropyl signal of the minor (*syn*) conformer is not split (Fig. 1), so this motion is probably still fast on the NMR timescale. Computations predict that the barrier for the phenyl–CO rotation in the *anti* conformer (7.4 kcal mol^{-1}) is higher than that of the fluorenyl–CO rotation barrier responsible for the conformer interconversion (*i.e.* 6.7 kcal mol^{-1}), whereas in the *syn* it is lower (4.8 kcal mol^{-1}; the structures of the transition states are displayed in Fig. S-1†). Accordingly, the phenyl–CO rotation barrier in the minor (*syn*) conformer could not be measured since it is too low to display a line splitting at −147 °C.[14] Although the rotation around the phenyl–CO bond in the major (*anti*) conformer is predicted to have the highest barrier (7.4 kcal mol^{-1}), its value cannot be measured, albeit for a different reason. This is because the two isopropyl groups of the *anti* form can exchange by a lower energy pathway (*anti* → *syn* → 180° Ph–CO rotation of the *syn* form → *anti*) and therefore the higher energy process (180° Ph–CO rotation of the *anti* form) cannot be detected.[15] A number of analogous cases where the higher of two barriers is NMR invisible have been reported.[16]

When a methyl group replaces the hydrogen in position 9 (see compound **2**), a steric effect is expected to destabilize the *anti* conformer with respect to the *syn* conformer. Indeed, DFT computations suggest that the energy of **2**-*anti* is much higher (6.8 kcal mol^{-1}) than that of **2**-*syn* (as in the case of **1**, the **2**-*syn* has a C_s and the **2**-*anti* has a C_1 symmetry). Accordingly, even at −165 °C, the NMR spectrum of **2** does not display any effect due to an exchange process, indicating that only one conformer is significantly populated. The DFT calculated barrier for the *syn–anti* interconversion is still quite high (7.4 kcal mol^{-1}), therefore the possibility of fast exchange at −165 °C, due to the ground states raising their energy, can be considered unlikely.

The *syn* structure was assigned to this conformer by an NOE experiment carried out at −80 °C irradiating the singlet of the methyl bonded to C9. Contrary to what was observed in **1**, the NOE enhancement of the *ortho* hydrogen signal of **2** is about 20 times *lower* than that of the fluorenyl hydrogens in position 1 and 8 (Fig. S-2†).

As in the spectrum of the *syn* conformer of **1**, the signals of the isopropyl groups of **2** do not split at low temperature, thus confirming that the Ph–CO rotation process is too fast to be NMR detected in the *syn* structure (the DFT-computed barrier predicted for this motion in **2**-*syn* is 4.4 kcal mol^{-1}).

Analogous behaviour is seen for the even more hindered derivative **3**, where there is again no evidence of an exchange between two conformers and only the *syn* conformer is populated. Computations suggest that the latter is more stable than the *anti* by 5.8 kcal mol^{-1}, and the single-crystal X-ray diffraction shows that only the *syn* form is present in the crystalline state (the dihedral angle Me_2C–C9–C–O is 19.5°, as in Scheme 3).

As for **2**, rotation about the Ph–CO bond in **3** is too fast to be NMR-detectable, and the CH multiplets of the isopropyl substituents in the phenyl ring remain isochronous at all attainable temperatures.

There is, however, another dynamic process which was detected here, *i.e.* the restricted rotation about the isopropyl–C9 bond. In the ^{1}H NMR spectrum, in fact, the methyl doublet of the single isopropyl substituent broadens considerably and eventually splits into two signals with a 1 : 1 intensity ratio (likewise the H-1,8 and other signals of the fluorene are split). Line-shape simulation of the methyl signals (Fig. 4) yields a barrier of 7.9 kcal mol^{-1} for this process (the same barrier is obtained from the corresponding ^{13}C spectrum and from the ^{1}H signal of the H-1,8 fluorene hydrogens, as in Fig. S-3 and S-4†, respectively). This value is matched by

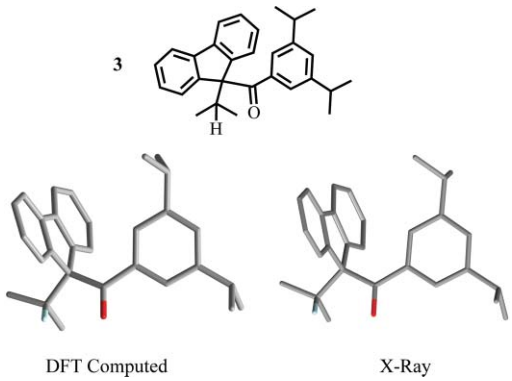

Scheme 3 Computed and X-ray structures of **3**. The hydrogens have been omitted, except that of the CH of the isopropyl group in position 9 of fluorene.

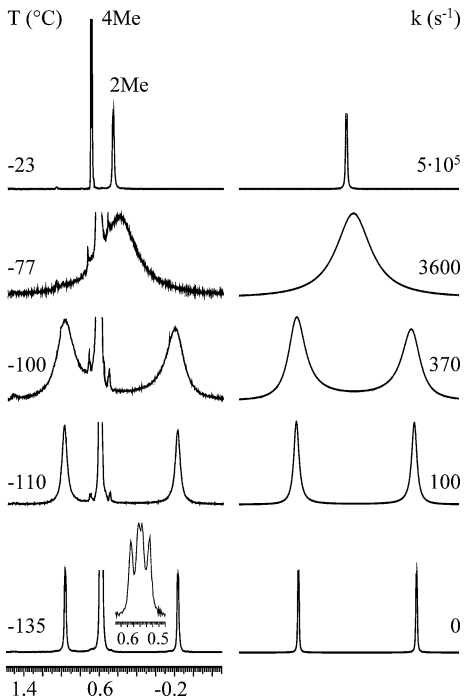

Fig. 4 Left: temperature dependence of the methyl signals (600 MHz) of the C9-isopropyl group of **3** in $CHF_2Cl/CHFCl_2$. The inset at −135 °C displays, on an expanded scale, the signals of the diastereotopic methyls of the two *meta*-isopropyls of the phenyl ring. Right: simulation of the methyl lines of the isopropyl bonded to C9, with the rate constants indicated.

DFT computations that predict a barrier of 7.8 kcal mol^{-1} for the isopropyl–C9 rotation (Table 1). When this process is frozen, the disposition of the isopropyl group is *gauche* with respect to the C=O moiety (the H–CMe_2–C9–CO dihedral angle is 52° in the computed and 50.6° in the X-ray structure), thus the molecule is chiral (C_1 symmetry, as in Scheme 2). For this reason, even in the presence of the mentioned rapid aryl–CO rotation (which mutually exchanges the two *meta*-isopropyl groups), the two methyls within a given *meta*-isopropyl group appear diastereotopic (*i.e.* they display two doublets, as in the inset in the bottom trace of Fig. 4) This is an example of the well known situation where the methyl groups of an isopropyl moiety behave as a probe of the molecular asymmetry.[17]

When the diisopropyl phenyl group, bonded to the carbonyl moiety, is replaced by the more hindered mesityl group, conformational preferences are modified. Whereas in **1–3** the phenyl ring is essentially coplanar, and that of fluorene is almost orthogonal with the plane containing the C=O group[18], in compound **4** computations indicate that the *anti* conformer is not an energy minimum, so only the *syn* conformer is populated. In both **4** and **5**[19] the mesityl and fluorene rings are disposed like a propeller with respect to the carbonyl plane. In the case of **4**, for instance, the Ph–CO dihedral angle, and that between the fluorene and the C=O plane, are 66° and 47°, respectively (see Fig. S-5†). The existence of a *syn* conformation is confirmed by a NOE experiment showing that the enhancement of the *ortho* methyl signal, on irradiating the H-1,8 signal, is lower than that of the C9 methyl signal. This result is consistent with the calculated structure (see Fig. S-6†).

On lowering the temperature, the signal of the *ortho* methyl groups of the mesityl ring of **4** splits into a 1 : 1 pair at −171 °C, whereas the other methyl signals do not (Fig. 5). At the same temperature the fluorenyl signal of H-1,8 is also split. These observations indicate that the molecule has adopted an asymmetric (and thus chiral) conformation, where the *ortho* methyl groups and the hydrogens pairs of fluorene are diastereotopic, in agreement with the structure predicted by computations. In addition, the trend of the computed chemical shifts reproduces the experimental values satisfactorily. From the line-shape simulations at three different temperatures, the barrier for exchanging the two *ortho* methyl signals of **4** is 4.4 ± 0.2 kcal mol^{-1}.

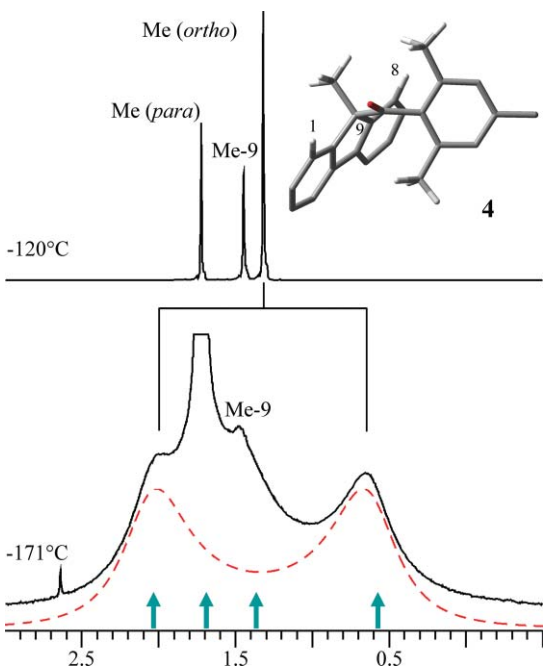

Fig. 5 ^{1}H NMR methyl signals of **4** (600 MHz in $CHF_2Cl/CHFCl_2$) showing the splitting of the *ortho* methyl line on lowering the temperature. The dashed trace corresponds to a simulation of the *ortho* lines obtained with a rate constant of 900 s^{-1}, and the arrows (moved upfield by 0.46 ppm) represent the DFT-computed chemical shifts.

The stereomutation pathway interconverting the enantiomeric conformations may be achieved by the passage through one or other of two transition states (see Fig. S-5†). In one, the mesityl

is coplanar with the carbonyl plane and orthogonal to fluorene, in the other is orthogonal to the C=O and parallel to fluorene. The former transition state has a calculated energy higher than the latter (the two computed values are 11.9 and 4.3 kcal mol^{-1}, respectively), but the higher barrier process is NMR-invisible as long as the second process, involving the lower energy transition state, is fast (the dynamic symmetry, in fact, is C_s). Only when the lower energy motion is slow on the NMR timescale are anisochronous signals for the diastereotopic *ortho* methyls seen.[16] The corresponding computed barrier (4.3 kcal mol^{-1}) matches well the measured value of 4.4 kcal mol^{-1} (Table 1). In both transition states, the normal mode corresponding to the calculated single imaginary frequency involves the displacement of both the mesityl and fluorene ring in opposite directions,[20] indicating the presence of a correlated motion of the fluorenyl–CO and CO–mesityl bonds, having the C=O as a pivot plane.

In compound **5** calculations once again predict that the only populated conformer is *syn* (the *anti* form is not even an energy minimum). The X-ray crystal structure of **5** (Scheme 4) shows a *syn* conformation, where the dihedral angle of the mesityl and of C=O is –80.6°, and that of the fluorene and C=O planes is 8.7° (–72° and 20° in the calculated structure, respectively). The compound crystallizes as a conglomerate ($Pna2_1$ group), although the absolute configuration could not be assigned in the crystal selected for the diffraction.

DFT computations, however, predict the existence of two different versions of the *syn* conformer, having very similar energies (the difference is only 0.2 kcal mol^{-1}). These differ in the rotational conformation about the C9-to-carbonyl bond. The more stable of these forms has the isopropyl methine hydrogen *trans* to the CO group (see Scheme 4), with the H-to-O distance equal to 3.40 Å. This corresponds to the X-ray structure, where this distance is 3.47 Å.

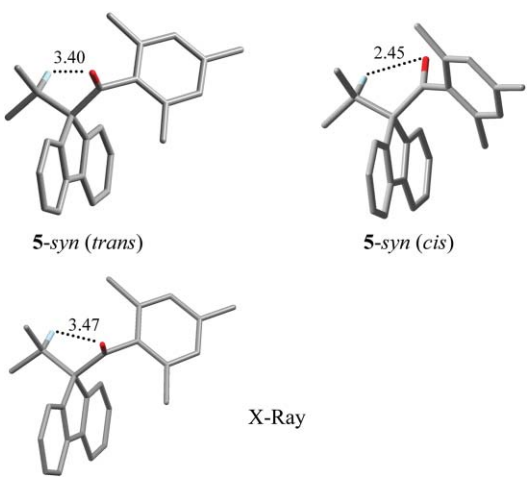

Scheme 4 Computed (top) and X-ray structure of **5**. The hydrogens have been omitted, except that of the CH of the isopropyl group in position 9 of fluorene (reported distances are in Å).

The less stable conformer has the methine hydrogen *cis* to the C=O group, with a shorter H-to-O distance (2.45 Å). Thus, in addition to the stereodynamic process observed in the analogous compound **3** (which likewise bears an isopropyl group bonded to C9), also the process leading to the observation of these two (*cis* and *trans*) conformers should be accessible to the low temperature NMR experiment.

The methyl region of the NMR spectrum (Fig. 6) shows that the lines of the isopropyl methyls broaden and split into a 1 : 1 pair at –148 °C. By analogy with compound **3**, this process corresponds to the isopropyl–C9 rotation and the experimentally measured barrier of 6.9 kcal mol^{-1} satisfactorily matches the calculated value of 6.2 kcal mol^{-1}, as in Table 1. At the same temperature the signal of the *ortho* methyls is also a 1:1 doublet (Fig. 6). The same set of rate constants successfully simulated the *ortho* methyl and isopropyl signals, indicating that these separate signals reflect the same dynamic process. The observed diastereotopicity of the *ortho* methyl groups suggests that the 180° rotation about the mesityl–CO bond, which exchanges them, is slow on the NMR timescale, and the computed barrier (13.0 kcal mol^{-1}) is much higher than the measured barrier of 6.9 kcal mol^{-1}. It is only when the frozen rotation of the isopropyl group (the rate-determining step) has made the molecule asymmetric, that the two *ortho* methyl groups become diastereotopic, due to their different positions with respect to the isopropyl moiety, even though the *cis–trans* interconversion is still fast. The higher barrier, corresponding to the mesityl–CO rotation, is thus NMR-invisible, and only the lower barrier (isopropyl–C9 rotation) can be measured.[16]

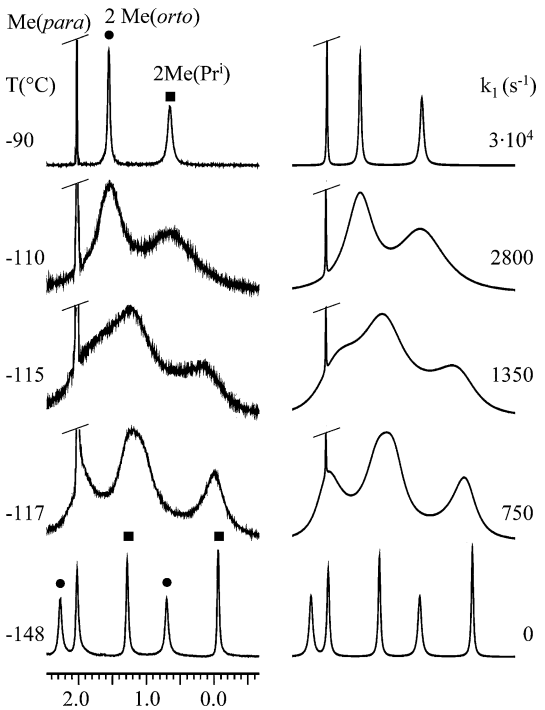

Fig. 6 Left: temperature dependence of the methyl signals (600 MHz) of the isopropyl groups of **5** in $CHF_2Cl/CHFCl_2$. Right: simulation obtained with the rate constants (k_1) indicated.

To detect the process which interconverts the *trans* and *cis* forms (Scheme 4) of the *syn* conformers of **5**, an even lower temperature is required. At the top of Fig. 7 three signals, due to the isopropyl methine hydrogen, to the lower field *ortho* methyl group and to the *para* methyl group, at –148 °C are displayed (at this temperature the rate constant k_1 for the isopropyl–C9 rotation is negligible, being lower than 2 s^{-1}). On further cooling to –159 °C, two additional signals, with a 10% intensity (1.82 and 3.10 ppm),

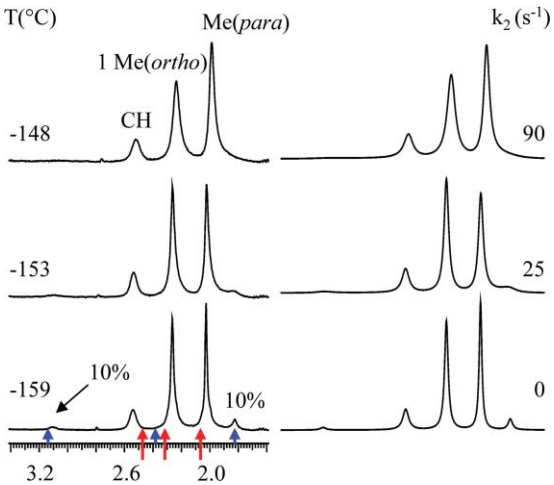

Fig. 7 Left: temperature dependence of the 1.6–3.4 ppm spectral region of **5** (600 MHz in $CHF_2Cl/CHFCl_2$) showing the presence of the signals of a minor (10%) form at –159 °C; the arrows (long for the major, short for the minor) represent the computed shifts (all moved 0.27 ppm upfield). Right: simulation obtained with the rate constants (k_2) indicated.

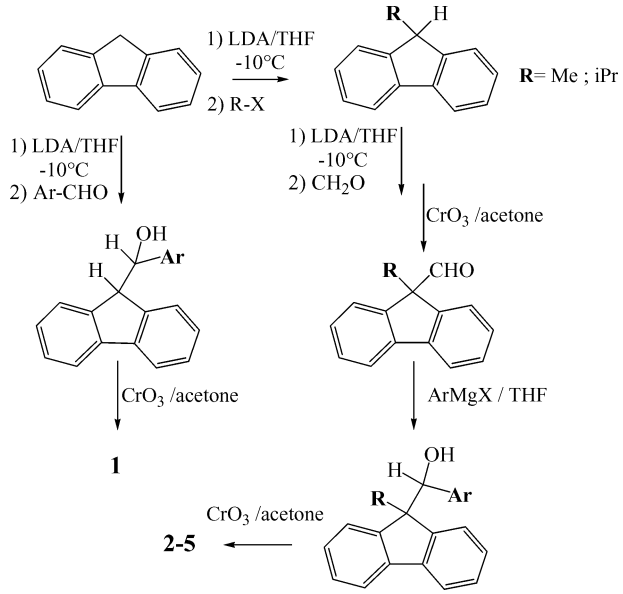

Scheme 5 Synthetic route to compounds **1–5**.

are detected. According to calculations and the X-ray structure, the more intense signals should correspond to the **5**-*syn* (*trans*) conformer of Scheme 4 and the less intense to the **5**-*syn* (*cis*).

Chemical shift calculations actually support this assignment: the methine hydrogen of the *cis* conformer is predicted to be at lower field with respect to the same hydrogen of the *trans*, whereas the Me(*para*) signal of the *cis* should be at higher field with respect to the *trans*, as experimentally observed (see Fig. 6).[21] The line shape simulation (obtained with the set of k_2 rate constants as in Fig. 7) yields a barrier of 6.0 kcal mol^{-1} for the interconversion of the more into the less stable of these two forms, the computed value being 4.8 kcal mol^{-1} (Table 1). The normal mode corresponding to the single imaginary frequency calculated in the low-energy transition state involves the displacement of both the mesityl and fluorene rings in opposite directions, indicating, once again, the presence of a correlated motion[20] of the two rings. The stereodynamic behaviour observed in **4** and **5** is analogous to that reported[22] in the case of the propeller-shaped dimesityl ketone.

The barriers determined for the dynamic processes in the course of this investigation are collected in Table 1.

Experimental section

Materials

Compound **1–5** were prepared according to Scheme 5. Full experimental details and spectroscopic data for the intermediates[5b,23–27] are reported in the ESI†.

(3,5-Diisopropylphenyl)-(9*H*-fluoren-9-yl)methanone (1). ^{1}H-NMR ($CDCl_3$, 600 MHz, 25 °C) δ 1.14 (6H, d, J = 6.9 Hz), 2.83 (2H, m, J = 6.9 Hz), 5.57 (1H, s), 7.18 (1H, t, J = 1.6 Hz), 7.29 (2H, dt, J = 7.7, 1.1 Hz), 7.39 (2H, d, J = 1.6 Hz), 7.42 (2H, d, J = 7.6 Hz), 7.45 (2H, dt, J = 7.7, 1.1 Hz), 7.87 (2H, d, J = 7.6 Hz). ^{13}C-NMR ($CDCl_3$, 150.8 MHz, 25 °C) δ 23.7 ($4CH_3$), 33.9 (2CH), 59.7 (CH), 120.4 (2CH), 124.7 (2CH), 125.2 (2CH), 127.5 (CH), 127.9 (2CH), 130.2 (CH), 136.1 (Cq), 141.5 (2Cq), 142.8 (2Cq), 149.0 (2Cq), 198.3 (CO). HRMS (EI) calculated for $C_{26}H_{26}O$: 354.1984; found 354.1982.

(3,5-Diisopropylphenyl)-(9-methylfluoren-9-yl)methanone (2). ^{1}H-NMR (CD_3CN, 600 MHz, 25 °C) δ 0.90 (6H, d, J = 6.9 Hz), 1.69 (3H, s), 2.61 (2H, septet, J = 6.9 Hz), 6.77 (2H, d, J = 1.6 Hz), 6.99 (1H, t, J = 1.6 Hz), 7.31 (2H, dt, J = 7.4, 1.1 Hz), 7.35 (2H, d, J = 7.4 Hz), 7.46 (2H, dt, J = 7.4, 1.2 Hz), 7.97 (2H, d, J = 7.6 Hz). ^{13}C-NMR (CD_3CN, 150.8 MHz, 25 °C) δ 24.3 ($4CH_3$), 25.4 (CH_3), 34.9 (2CH), 64.3 (Cq), 122.4 (2CH), 124.9 (2CH), 125.1 (2CH), 129.5 (2CH), 129.6 (2CH), 130.6 (CH), 137.9 (Cq), 142.1 (2Cq), 149.9 (2Cq), 150.6 (2Cq), 201.3 (CO). HRMS (EI) calculated for $C_{27}H_{28}O$: 368.2140; found 328.2141.

(3,5-Diisopropylphenyl)-(9-isopropylfluoren-9-yl)methanone (3). Mp 77–79 °C. ^{1}H-NMR (CD_3CN, 600 MHz, 25 °C) δ 0.67 (6H, d, J = 6.9 Hz), 0.92 (12H, d, J = 6.9 Hz), 2.58 (2H, septet, J = 6.9 Hz), 3.26 (1H, septet, J = 6.9 Hz), 6.70 (2H, d, J = 1.6 Hz), 6.86 (1H, t, J = 1.6 Hz), 7.21 (2H, dt, J = 7.6, 1.1 Hz), 7.31 (2H, d, J = 7.6 Hz), 7.38 (2H, dt, J = 7.6, 1.1 Hz), 7.83 (2H, d, J = 7.6 Hz). ^{13}C-NMR (CD_3CN, 150.8 MHz, 25 °C) δ 18.3 ($2CH_3$), 23.8 ($4CH_3$), 34.0 (2CH), 35.3 (CH), 71.4 (Cq), 120.3 (2CH), 123.8 (2CH), 125.6 (2CH), 127.7 (2CH), 128.0 (2CH), 128,8 (CH), 137.9 (Cq), 142.0 (2Cq), 146.7 (2Cq), 148.1 (2Cq), 202.3 (CO). HRMS (EI) calculated for $C_{29}H_{32}O$: 396.2453; found 396.2456.

Mesityl-(9-methylfluoren-9-yl)methanone (4). ^{1}H-NMR (CD_3CN, 600 MHz, 25 °C) δ 1.70 (6H, s), 1.84 (3H, s), 2.15 (3H, s), 6.65 (2H, s), 7.23 (2H, dt, J = 7.6, 1.1 Hz), 7.38 (2H, dt, J = 7.6, 1.1 Hz), 7.49 (2H, d, J = 7.6 Hz), 7.78 (2H, d, J = 7.6 Hz). ^{13}C-NMR (CD_3CN, 150.8 MHz, 25 °C) δ 20.2 ($2CH_3$), 21.3 (CH_3), 28.4 (CH_3), 65.5 (Cq), 121.3 (2CH), 126.5 (2CH), 128.8 (2CH), 129.2 (2CH), 129.4 (2CH), 133.8 (CH), 139.3 (2Cq), 140.7 (Cq), 141.5 (2Cq), 148.5 (2Cq), 213.2 (CO). HRMS (EI) calculated for $C_{24}H_{22}O$: 326.1671; found 326.1676.

Mesityl-(9-isopropylfluoren-9-yl)methanone (5). Mp 206–208 °C. ^{1}H-NMR (CD_3CN, 600 MHz, 25 °C) δ 0.75 (6H, d,

J = 6.7 Hz), 1.68 (6H, s), 2.15 (3H, s), 2.97 (1H, septet, J = 6.7 Hz), 6.62 (2H, s), 7.21 (2H, dt, J = 7.6, 1.1 Hz), 7.38 (2H, dt, J = 7.6, 1.1 Hz), 7.44 (2H, d, J = 7.6 Hz), 7.77 (2H, d, J = 7.6 Hz). ^{13}C-NMR (CD_3CN, 150.8 MHz, 25 °C) δ 17.9 ($2CH_3$), 18.9 ($2CH_3$), 20.1 (CH_3), 36.5 (CH), 72.7 (Cq), 119.7 (2CH), 126.5 (2CH), 127.2 (2CH), 128.0 (2CH), 128.2 (2CH), 133.1 (CH), 138.0 (2Cq), 139.7 (Cq), 141.7 (2Cq), 144.7 (2Cq), 210.5 (Cq). HRMS (EI) calculated for $C_{26}H_{26}O$: 354.1984; found 354.1982.

NMR spectroscopy

The spectra were recorded at 600 MHz for ^{1}H and 150.8 MHz for ^{13}C on a Varian Inova spectrometer. Low temperature spectra were obtained with a customized dual band direct probe. The assignments of the ^{1}H and ^{13}C signals were obtained by bi-dimensional experiments (edited-gsHSQC[28] and gsHMBC[29]). The NOE experiments were obtained by means of the DPFGSE-NOE[30] sequence. To selectively irradiate the desired signal, a 50 Hz wide shaped pulse was calculated with a refocusing-SNOB shape[31] and a pulse width of 37 ms. The mixing time was set to 1.0 s. The samples for obtaining spectra at temperatures lower than −100 °C were prepared by connecting to a vacuum line the NMR tubes containing the compound and some C_6D_6 for locking purposes and condensing therein the gaseous CHF_2Cl and $CHFCl_2$ (4 : 1 v/v) under cooling with liquid nitrogen. The tubes were subsequently sealed *in vacuo* and introduced into the cooled probe of the spectrometer. Temperature calibrations were performed before the experiments, using a Cu/Ni thermocouple immersed in a dummy sample tube filled with isopentane, and under conditions as nearly identical as possible. The uncertainty in the temperatures was estimated from the calibration curve to be ±2 °C. Low temperature ^{13}C spectra were acquired without spinning, with a sweep width of 38000 Hz, a pulse width of 4.9 μs (70° tip angle), and a delay time of 2.0 s. Proton decoupling was achieved with the standard Waltz-16 sequence. A line broadening function of 1–5 Hz was applied to the FIDs before Fourier transformation. Usually 512 to 1024 scans were acquired. The line shape simulations were performed by means of a PC version of the QCPE program DNMR 6 no. 633, Indiana University, Bloomington, IN.

Computational details

Geometry optimizations were usually carried out at the B3LYP/6-31G(d) level by means of the Gaussian 03 series of programs[8] and Xeon™ multiprocessor servers running Scientific Linux 5.2-X86_64 as the operating system. In the case of **1**, full geometry optimization was carried out also at the B3LYP/6-311++G(2d,p)[32], PBE1PBE/6-31G(d)[33], M05–2X/6-31G(d)[13h], RHF(full)/6-31G(d) and RHF/cc-pVDZ levels of theory. Single-point calculations were obtained at the MP2(full)/6-31G(d)//B3LYP/6-311++G(2d,p) and CISD/6-31G(d)//B3LYP/6-311++G(2d,p). The standard Berny algorithm in redundant internal coordinates and default criteria of convergence were employed in all the calculations. Harmonic vibrational frequencies were calculated for all the optimized stationary points, For each ground state the frequency analysis showed the absence of imaginary frequencies, whereas each transition state showed a single imaginary frequency. Visual inspection of the corresponding normal mode was used to confirm that the right transition state had been found. NMR chemical shift calculations were obtained with the GIAO[34] method at the B3LYP/6-311++G(2d,p)//B3LYP/6-31G(d) level. TMS, calculated at the same level of theory, was used as reference to scale the absolute shielding value.

Acknowledgements

L.L. and A.M. received financial support from the University of Bologna (RFO) and from MUR-COFIN 2005, Rome (national project "Stereoselection in Organic Synthesis"). The authors thanks one anonymous referee for helpful suggestions.

References and notes

1 M. Oki, *Applications of Dynamic NMR Spectroscopy to Organic Chemistry*, VCH Publishers, Deerfield Beach, FL, 1985, p. 211.
2 A. Nishida, M. Takeshita, S. Fujisaki and S. Kajigaeshi, *Bull. Soc. Chim. Jpn.*, 1988, **61**, 1195–1200.
3 A. Nishida, Y. Akagawa, S. Shirakawa, S. Fujisaki and S. Kajigaeshi, *Can. J. Chem.*, 1991, **69**, 615–619.
4 J. Vicario, A. Meetsma and B. L. Feringa, *Chem. Commun.*, 2005, 5910–5012; J. Vicario, M. Walko, A. Meetsma and B. L. Feringa, *J. Am. Chem. Soc.*, 2006, **128**, 5127–51235.
5 (*a*) D. Casarini, L. Lunazzi and A. Mazzanti, *J. Org. Chem.*, 2008, **73**, 2811–2818; (*b*) D. Casarini, L. Lunazzi and A. Mazzanti, *J. Org. Chem.*, 2008, **73**, 6382–6385.
6 *MMFF conformational search implemented in TITAN 1.0.5*, Wavefunction Inc, Irvine, CA.
7 *MMX force field as in the program PC-Model V. 7.5*, Serena Software, Bloomington, IN.
8 M. J. Frisch, G. W. Trucks, H. B. Schlegel, G. E. Scuseria, M. A. Robb, J. R. Cheeseman, J. A. Montgomery, Jr., T. Vreven, K. N. Kudin, J. C. Burant, J. M. Millam, S. S. Iyengar, J. Tomasi, V. Barone, B. Mennucci, M. Cossi, G. Scalmani, N. Rega, G. A. Petersson, H. Nakatsuji, M. Hada, M. Ehara, K. Toyota, R. Fukuda, J. Hasegawa, M. Ishida, T. Nakajima, Y. Honda, O. Kitao, H. Nakai, M. Klene, X. Li, J. E. Knox, H. P. Hratchian, J. B. Cross, V. Bakken, C. Adamo, J. Jaramillo, R. Gomperts, R. E. Stratmann, O. Yazyev, A. J. Austin, R. Cammi, C. Pomelli, J. Ochterski, P. Y. Ayala, K. Morokuma, G. A. Voth, P. Salvador, J. J. Dannenberg, V. G. Zakrzewski, S. Dapprich, A. D. Daniels, M. C. Strain, O. Farkas, D. K. Malick, A. D. Rabuck, K. Raghavachari, J. B. Foresman, J. V. Ortiz, Q. Cui, A. G. Baboul, S. Clifford, J. Cioslowski, B. B. Stefanov, G. Liu, A. Liashenko, P. Piskorz, I. Komaromi, R. L. Martin, D. J. Fox, T. Keith, M. A. Al-Laham, C. Y. Peng, A. Nanayakkara, M. Challacombe, P. M. W. Gill, B. G. Johnson, W. Chen, M. W. Wong, C. Gonzalez and J. A. Pople, *GAUSSIAN 03 (Revision E.01)*, Gaussian, Inc., Wallingford, CT, 2004.
9 The average distances used for the comparison with the NOE effects were derived from the DFT-computed structures by means of the relationship $\langle r^{-6}\rangle^{-1/6}$, according to: T. D. W. Claridge, *High-Resolution NMR Techniques in Organic Chemistry*, Pergamon, Oxford, 1987, p. 303. In **1**-*anti* these distances are 3.07 Å (between H-9 and H-1,8) and 2.25 Å (between H-9 and H_{ortho}). In **1**-*syn* the same distances are 3.07 and 4.08 Å, respectively. Their ratios (elevated to the 6th power) are 6.4 : 1 in **1**-*anti* whereas they are reversed to 1 : 5.5 in **1**-*syn*.
10 The 94 : 6 ratio measured at −147 °C (Fig. 1) corresponds, approximately, to a 86 : 14 ratio at −80 °C. Therefore, the observed NOE effects at −80 °C are mainly due to the geometry of the more populated conformer. However, the presence of a non-negligible amount of the minor conformer should account for the difference between the calculated NOE ratio for a 100% population of **1**-*anti* (*i.e.* 6.4 : 1) and the experimental value (*i.e.* 3.1 : 1). In particular, the observed 3.1 NOE ratio would be accounted for by an *anti*-to-*syn* proportion of 73 : 27: such a proportion is in acceptable agreement with the above mentioned 86 : 14 ratio.
11 Assignment unambiguously established by means of NOE experiments obtained by irradiation of isopropyl CH and methyl signals.

12 The latter experiment has been performed in order to exclude the possibility that differences on T_1 values could significantly affect the NOE ratios.
13 (*a*) C. E. Check and T. M. Gilbert, *J. Org. Chem.*, 2005, **70**, 9828–9834; (*b*) M. D. Wodrich, C. Corminbouef and P. v. R. Schleyer, *Org. Lett.*, 2006, **8**, 3631–3634; (*c*) P. R. Shreiner, A. A. Fokin, R. A. J. Pascal and A. De Mejere, *Org. Lett.*, 2006, **8**, 3635–3638; (*d*) S. Grimme, *Angew. Chem. Int. Ed.*, 2006, **45**, 4460–4464; (*e*) Y. Zhao and D. G. Truhlar, *Org. Lett.*, 2006, **8**, 5753–5755; T. A. Rokob, A. Hamza and I. Pßpai, *Org. Lett.*, 2007, **9**, 4279–4282; (*f*) P. R. Shreiner, *Angew. Chem. Int. Ed.*, 2007, **46**, 4217–4219; (*g*) M. D. Wodrich, C. S. Wannere, Y. Mo, P. D. Jarowski, K. N. Houk and P. v. R. Schleyer, *Chem. Eur. J.*, 2007, **13**, 7731–7744; (*h*) Y. Zhao and D. G. Truhlar, *Acc. Chem. Res.*, 2008, **41**, 157–167; (*i*) T. Schwabe and S. Grimme, *Acc. Chem. Res.*, 2008, **41**, 569–579; (*j*) M. D. Wodrich, D. F. Jana, P. v. R. Schleyer and C. Corminbouef, *J. Phys. Chem. A*, 2008, **112**, 11495–11500.
14 On further lowering of the temperature, the viscosity makes the intrinsic line width too broad to detect the possible splitting of the lines in the minor conformer.
15 As proof of this feature the simulation of Fig. 3 could be obtained using solely the rate constant for the interconversion of the major into the minor signals, without the introduction of a rate constant which directly exchanges the 1 : 1 signals of the major conformer, so the latter rate cannot be determined by NMR.
16 W. R. Jackson and W. B. Jennings, *Tetrahedron Letters*, 1974, **15**, 1837–1838; J. E. Anderson, D. Casarini, A. J. Ijeh and L. Lunazzi, *J. Am. Chem. Soc.*, 1997, **119**, 8050–8057; D. Casarini, L. Lunazzi, A. Mazzanti and E. Foresti, *J. Org. Chem.*, 1998, **63**, 4746–4754; L. Lunazzi, A. Mazzanti and A. Álvarez Muñoz, *J. Org. Chem.*, 2000, **65**, 3200–3206.
17 K. Mislow and M. Raban, *Top. Stereochem.*, 1967, **1**, 1; W. B. Jennings, *Chem. Rev.*, 1975, **75**, 30; E. L. Eliel, *J. Chem. Ed.*, 1980, **57**, 52.
18 The computed angles are 1° and 90°; 0° and 90°; 21° and 68° in **1**, **2** and **3**, respectively.
19 The mesityl derivative corresponding to **1** could not be studied because on synthesis it immediately forms its 9,9′-dimer.
20 This results from a visual inspection of the normal mode by an appropriate computer program: R. Dennington II, T. Keith and J. Millam, *GaussView* (Version 4.1), Semichem, Inc., Shawnee Mission, KS, 2007.
21 The expected third 10% signal is not observed because it is overlapped by the line at 2.28 ppm. A satisfactory line shape simulation could be obtained only if the 90% Me(*para*) line at 2.02 ppm exchanges with the hidden 10% line at 2.28 ppm, and the downfield 90% Me(*ortho*) line at 2.28 ppm exchanges with the 10% line at 1.82 ppm. The major signal at 2.54 ppm is that of the methine hydrogen, which exchanges with the corresponding minor signal at 3.10 ppm (Fig. 7).
22 S. Grilli, L. Lunazzi, A. Mazzanti, D. Casarini and C. Femoni, *J. Org. Chem.*, 2001, **66**, 488–495 and references quoted therein.
23 V. Diemer, H. Chaumeil, A. Defoin, A. Fort, A. Boeglin and C. Carré, *Eur. J. Org. Chem.*, 2006, 727–2738; H. R. Liu, P. T. Gomes, S. I. Costa, M. T. Duarte, R. Braquinho, A. C. Fernandes, J. C. W. Chien, R. P. Singh and M. M. Marques, *J. Organomet. Chem.*, 2005, **690**, 1314–1323.
24 P. Müller and J. Blanc, *Helv. Chim. Acta*, 1979, **62**, 1980–84.
25 J. Perumattam, C. Shao and W. L. Confer, *Synthesis*, 1994, 1181–1184; F. A. L. Anet and P. M. G. Bavin, *Can. J. Chem.*, 1956, **34**, 1756–1759.
26 F. Brisse, G. Durocher, S. Gauthier, D. Gravel, R. Marques, C. Vergelati and B. Zelent, *J. Am. Chem. Soc.*, 1986, **109**, 6759–6586; J.-Y. Cho, B. Domercq, S. Barlow, K. Y. Suponitsky, J. Li, T. V. Timofeeva, S. C. Jones, L. E. Hayden, A. Kimyonok, C. R. South, M. Weck, B. Kippelen and S. R. Marder, *Organometallics*, 2007, **27**, 4816–4829.
27 S. Fujiwara, T. Matsuya, H. Maeda, T. Shin-ike, N. Kambe and N. Sonoda, *J. Org. Chem.*, 2001, **66**, 2183–2185.
28 S. A. Bradley and K. Krishnamurthy, *Magn. Reson. Chem.*, 2005, **43**, 117; E. Kupče and R. Freeman, *J. Magn. Reson. A*, 1996, **118**, 299–303; W. Willker, D. Leibfritz, R. Kerssebaum and W. Bermel, *Magn. Reson. Chem.*, 1993, **31**, 287–292.
29 R. E. Hurd and B. K. John, *J. Magn. Reson.*, 1991, **91**, 648–653.
30 K. Stott, J. Stonehouse, J. Keeler, T.-L. Hwand and A. J. Shaka, *J. Am. Chem. Soc.*, 1995, **117**, 4199; K. Stott, J. Keeler, Q. N. Van and A. J. Shaka, *J. Magn. Reson.*, 1997, **125**, 302; Q. N. Van, E. M. Smith and A. J. Shaka, *J. Magn. Reson.*, 1999, **141**, 191; see also: T. D. W. Claridge, *High Resolution NMR Techniques in Organic Chemistry*, Pergamon, Amsterdam, 1999, pp. 320–322.
31 E. Kupče, J. Boyd and I. D. Campbell, *J. Magn. Reson. B*, 1995, **106**, 300–303.
32 P. J. Stephens, F. J. Devlin, C. F. Chabalowski and M. J. Frisch, *J. Phys. Chem.*, 1994, **98**, 11623–11627; A. D. Becke, *J. Chem. Phys.*, 1993, **98**, 5648–5652; C. Lee, W. Yang and R. G. Parr, *Phys. Rev., B*, 1988, **37**, 785–789.
33 J. P. Perdew, K. Burke and M. Ernzerhof, *Phys. Rev. Lett.*, 1996, **77**, 3865–3868.
34 K. Wolinski, J. F. Hilton and P. Pulay, *J. Am. Chem. Soc.*, 1990, **112**, 8251–8260.

